Impact of wave interactions effects on energy absorption in large arrays of Wave Energy Converters

Bruno Borgarino, Aurélien Babarit, Pierre Ferrant

Impact of wave interactions effects on energy absorption in large arrays of wave energy converters

B. Borgarino*, A. Babarit, P. Ferrant

Laboratoire de Mecanique des Fluides (LMF), Ecole Centrale de Nantes, France

This paper presents a parametric study on arrays of wave energy converters (WECs). Its goal is to assess the influence of interactions between bodies on the overall yearly energy production of the array. Generic WECs (heaving cylinder and surging barge) are considered. Nine to twenty-five WECs are installed along regular square and triangular grids; the influence of the separating distance between the WECs is investigated. Results show that constructive and destructive interactions compensate each other over the considered range of wave periods. The influence of the separating distance can be limited, especially if the damping of the power take-off is tuned properly, and if the WECs have a large bandwidth. It is found that grouping the devices into arrays have generally a constructive effect. Diffracted and radiated waves in the array lead to a sufficient increase in the energy absorption which overcomes the reduction due to masking effects.

1. Introduction

Wave energy converters (WECs) are likely to be deployed in large arrays of tens of devices. Within the WEC array, interactions between the bodies will occur, due to diffracted waves and waves radiated by the motions of each body. These interactions can strongly impact the overall power production of the array, being either constructive or destructive, depending on the geometry of the bodies, their positions within the array, the wavelength and the control strategy. Assessing the effects of wave interactions is thus critical when designing a WEC array.

This topic has motivated many research studies over the years, based on different approaches. In their early works, Budal (1977), Falnes and Budal (1982), Falnes (1984), Thomas and Evans (1981) built analytical models of WEC arrays and proved the possibility of constructive interactions. More recently, Garnaud and Mei (2009) derived a theory for dense arrays of small WECs.

Boundary element methods (BEM), based on linear potential flow theory, permit to numerically solve the motions of WECs having an arbitrary shape, with full consideration of wave interactions between bodies. Parametric studies using these tools can be found in Justino and Clement (2003), Ricci et al. (2007), Babarit (2010) for example. However, because of limitations in computation time, only a few WEC array configurations can be tested, with a limited number of bodies. BEM results obtained for a specific WEC array configuration are often used to determine the best power take-off (PTO) strategy (De Backer et al., 2009; Cruz et al., 2009; Bellew et al., 2009). Folley and Whittaker (2009) investigated the coupling of the WECs array layout with the control strategy.

Other studies question the optimal positioning of devices in the WEC array without using BEM: Filtzgerald and Thomas (2007) derived an optimization problem to build optimal WEC arrays, using the small body approximation to get the motions of the bodies. Child and Venugopal (2009) applied the interaction theory to solve interactions within the WEC array. This theory expresses the potential of the incident, radiated and diffracted wave fields as the product of two vectors: a vector representing all the diffracted and radiated waves than can occur around a cylinder, and a vector of weighting coefficients. Child and Venugopal (2009) numerically determined optimal WEC arrays for different objectives, using a genetic algorithm and parabolic intersection methods.

This paper assesses the influence of separating distances between generic point-absorber WECs. It is based on the model presented in Babarit (2010), but uses a BEM tool specifically accelerated for WEC arrays problems. WEC arrays of 9–25 heaving cylinders and surging barges are considered. They are built according to regular grids and the separating distance between WECs is investigated. Most studies on WEC arrays concern closely spaced floating bodies; however, Babarit (2010) showed that interactions between WECs can be significant even at large distances (2000 m). Consequently distances from 10 to 50 times the characteristic length of a WEC are considered here. All the bodies in the WEC array have the same geometry and power take-off. Two simple strategies are tested for tuning the PTO damping. The yearly averaged power of the WEC array at a specific

* Corresponding author.
E-mail address: Bruno.Borgarino@ec-nantes.fr (B. Borgarino).

site is investigated depending on these parameters. The results give an insight on the role of interactions within the WEC array, and provide simple guidelines to apply when designing a WEC array.

2. Methods

2.1. Equation of motions

The equation of motions for a set of floating bodies is established in the frame of linear potential flow theory. The hypotheses are the following:

- The fluid is assumed to be inviscid and incompressible.
- The flow is irrotationnal.
- Bodies motions are small compared to their characteristic length.
- The amplitude of the wave is small compared to the wavelength.

In this study, no moorings are considered. The PTO is modelled as a linear damping system (b_{pto}) in parallel with a linear spring (k_{pto}). The bodies have only one mode of motion, along the working direction of the PTO. For a system of several floating bodies, excited by waves of amplitude 1 m and of frequency ω:

$$(M+AM(\omega))\ddot{X}+(B_{PTO}+B(\omega))\dot{X}+(K_H+K_{PTO})X=F_{ex}(\omega) \quad (1)$$

X, $(\dot{X})$ and $(\ddot{X})$ are functions of ω in Eq.1
with:

- N_b the total number of floating bodies in the WEC array.
- $X(x_1,\ldots,x_{N_b})$ the position vector of the WEC array according to the allowed mode of motion. $X=\Re(\overline{X}e^{i\omega t})$. X, $(\dot{X})$, $(\ddot{X})$ are functions of ω
- M is the mass matrix of the system (diagonal).
- K_H is the hydrostatic matrix of the system (diagonal).
- K_{PTO} and B_{PTO} are the matrices related to the stiffness and the damping of the PTO (diagonal). $\forall i$, $K_{PTO_{ii}}=k_{pto}$, $B_{PTO_{ii}}=b_{pto}$.
- $AM(\omega)$ and $B(\omega)$ are the hydrodynamic added-mass matrix and damping matrix of the system. As the WECs interact through the waves they radiate, these matrices are not diagonal. It can be demonstrated that $\forall(i,j)$, $AM_{ij}(\omega)=AM_{ji}(\omega)$ and $B_{ij}(\omega)=B_{ji}(\omega)$.
- $F_{ex}(\omega)=\Re(\overline{F}_{ex}e^{i\omega t})$ is the excitation force, resulting from the addition of the incident wave field and the wave field diffracted by the WEC array.

In regular incident waves, the power extracted at each wave frequency by the whole WEC array is

$$p(\omega)=\sum_{i=1}^{N_b}p_i(\omega) \quad (2)$$

with p_i the power extracted by the individual body i:

$$p_i(\omega)=\tfrac{1}{2}b_{pto}\omega^2|X_i|^2 \quad (3)$$

X is a function of ω. Because of linearity, the extracted power of a body i in irregular incident waves is given by:

$$P_i(H_s,T_p)=\int_0^{\infty}S(T_p,H_s,\omega)p_i(\omega)\,d\omega \quad (4)$$

where S is the standard JONSWAP spectrum, H_s the significant wave height, and T_p the peak period. For all sea states the chosen frequency spreading parameter is $\gamma=3.3$. The yearly averaged power of a body i, given the probability of occurrence $C(H_s,T_p)$ of the sea state (H_s,T_p) is calculated by:

$$Pyr_i=\langle P_i\rangle=\sum_{H_s,T_p}C(H_s,T_p)P_i(H_s,T_p) \quad (5)$$

As a consequence Pyr^i is site specific.

2.2. Characteristics of the WEC arrays

2.2.1. Considered wave energy converters

Geometries: As in Babarit (2010), two different types of WECs are considered: a heaving cylinder and a surging barge (rectangular shaped body). Both bodies have the same water displacement (785 m^3), the same width facing the incident wave (10 m) and the same draft (10 m). The length of the surging barge in the direction parallel to the wave propagation is 7.85 m. The WECs have all motions other than their working direction (heave or surge) ideally restricted. Consequently, only one radiation problem per body is solved.

Power take-off: All the bodies of the WEC array have the same PTO characteristics. The surging barge PTO stiffness k_{pto} is chosen so that the heaving cylinder and the surging barge have the same resonant frequency ($T_0\approx 7.3$ s). In this paper, the PTO damping is tuned in two different ways:

- The value $b_{pto\ year}$ which permits the highest energy production of an isolated WEC over the year is chosen. This value is simply found by changing values of b_{pto}.
- $b_{pto}=b_{pto\ \omega_0}$ is taken equal to the hydrodynamic damping $B(\omega_0)$ of an isolated WEC at its resonant frequency ω_0, as suggested in Falnes (2002).

The first strategy takes into account the available wave resource. It permits to simply tune a generic WEC to the local wave climate, independently of its mass and geometry. The second strategy will permit to maximize power production at the resonant frequency, and is in a sense 'WEC specific'. The value of $b_{pto\ year}$ is found larger than the value of $b_{pto\ \omega_0}$ (Table 1). Logically, the motion amplitudes are smaller (Fig. 1). Moreover, $b_{pto}=b_{pto\ year}$ gives the WECs a larger bandwidth and shifts the power curves toward the most energetic wave periods.

2.2.2. Parameters of the WEC arrays

The WEC array is made of a square number of bodies (9–25) installed along a regular grid described by the couple of separating distances in the horizontal space (dx,dy), and having the same number of rows and columns. "Row" stands for a subset of bodies facing the incident waves. "Column" stands for a subset of bodies roughly aligned along the direction of wave propagation; the waves come from the $-x$ direction (from the left on Fig. 2). In this article, "square-based array" means that $dx=dy$. "Triangle-based array" means that $dx=(\sqrt{3}/2)dy$ and that each row is shifted of $\pm dy/2$ (the grid is then based on equilateral triangles). These two configurations permit to characterize the WEC array by one parameter dx only (see Fig. 2). Separating distances dx with values smaller than 100 m were not considered. It is believed that such short distances are not likely to happen, due to mooring issues. The WEC array maximum length is set to 1 km, which gives the maximum value of dx depending on the number of rows. The bodies in the WEC array are labelled from 1 to N_b according to the index of their row and column, as follows: body index = (row index−1) × number of bodies per row + column index. On Fig. 2, as the waves come from the left, the 1st row is the set of three bodies situated at $x=0$. Thus, body 7 on Fig. 2 is the one situated at $(x,y)=(200,0)$, on the 3rd

Table 1
PTO characteristics of the considered WECs.

WEC	Stiffness k_{pto} (kN/m)	Damping $b_{pto\ \omega_0}$ (kN.s/m)	Damping $b_{pto\ year}$ (kN s/m)	Resonant wave Period T_0 (s)
Cylinder	0.0	25.9	336.1	7.29
Barge	1402.1	159.9	444.2	7.29

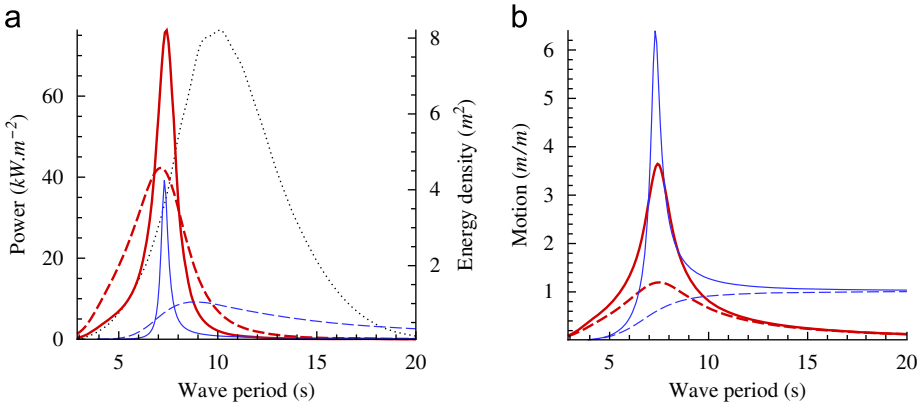

Fig. 1. WECs responses depending on the PTO strategy. Thick lines, surging barge; thin lines, heaving cylinder; solid line, $b_{pto} = b_{pto\ \omega_0}$; dashed line, $b_{pto} = b_{pto\ yr}$; dotted line, energy density. (a) Power and (b) motions.

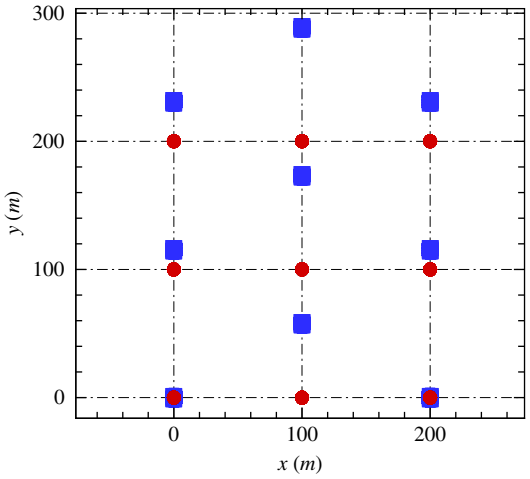

Fig. 2. 9-body arrays built with separating distance $dx = 100$ m. Circles, square-based array of cylinders; squares, triangle-based array of barges. The waves come from the $-x$ direction (left).

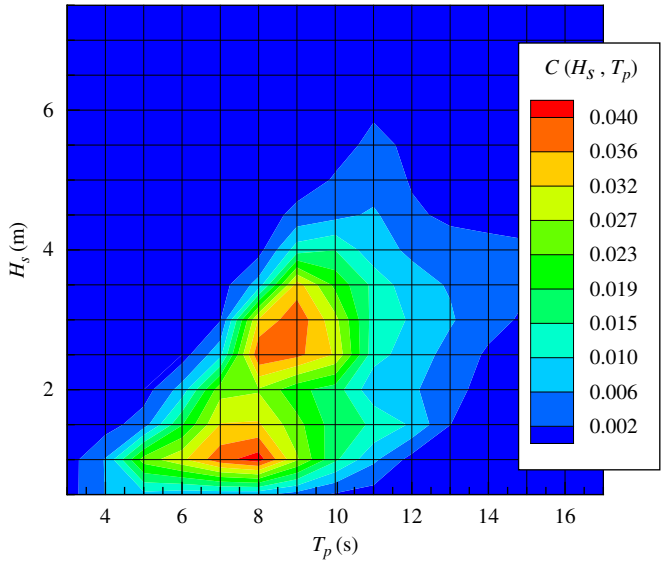

Fig. 3. Wave scatter diagram for Yeu island. Color layers: probability of occurrence $C(H_s,T_p)$. (For interpretation of the references to color in this figure legend, the reader is referred to the web version of this article.)

row and the 1st column. Computations are run on the wave data from Yeu island (France) represented on Fig. 3. The water depth at this site is about 50 m; the bathymetry is nearly flat.

Table 2
Characteristic computational times, in hours. The number of problems is the number of radiation/diffraction problems, multiplied by the number of investigated wave periods.

Parc	No. of problems	Wall clock time (h)
9 cylinders	1450	0.472
16 cylinders	2465	1.708
25 cylinders	3770	4.750
9 barges	1870	5.056
16 barges	3179	8.194
25 barges	4862	27.694

2.3. Numerical model

The resolution of Eq. (1) has been implemented in Fortran programming language by Babarit (2010). The quantities $AM(\omega)$, $B(\omega)$ and $\overline{F}_{ex}(\omega)$ are computed using Aquaplus (Delhommeau, 1993), a diffraction/radiation BEM software developed at LMF for the past thirty years. Aquaplus has recently been enhanced to run fast and low memory intensive computations on large WEC arrays (up to 50 floating bodies). The hydrodynamic problems resolution is accelerated by a General Minimum Residual (GMRes) solver (Saad and Schultz, 1986) combined with a simplified Fast Multipole Algorithm (Greengard, 1988). This implementation is fully described by Borgarino et al. (submitted for publication). It is a recent improvement, which so far can only model infinite water depth problems. Thus, the results are not fully representative of the Yeu island situation. This is not an issue, as the goal of this study is not to design an array for this specific site, but to identify the main tendencies occurring in WECs arrays given a set of wave data.

The surfaces of the bodies are modelled by 260 panels (cylinder) or 272 panels (barge). Convergence studies were conducted to verify that these meshes provide accurate enough representations of the bodies.

Table 2 gives an overview of the "wall clock time" needed to solve all the radiation/diffraction problems (with one degree of freedom per body, and one wave incidence angle) on the considered wave period range, for various arrays. The differences between the cylinder case and the barge case are due to the convergence of the GMRes needing more iterations in the barge case.

3. Results

This section presents results on yearly energy production when changing the separating distance dx in the WEC array. The distance step is 10 m.

Different indicators are used: the q-factor q, the q_{mod}-factor (modified q-factor) and the yearly power output Pyr. At a given wave frequency ω, for a body i,

$$q(\omega) = \frac{p_i(\omega)}{p_0(\omega)} \tag{6}$$

with $p_0(\omega)$ the power output of an isolated WEC, and $p_i(\omega)$ the power output of the ith body in the array (see Eq. (3)). When $q(\omega) > 1$, constructive interactions occur: for instance, wave focusing effects result into an increase of the power absorption per WEC. When $q(\omega) < 1$, the interactions are destructive: masking effects diminish the overall power absorption of the array. Babarit (2010) introduced the q_{mod}-factor, which only takes into account significant wave interactions, occurring at the frequencies where most of the power is produced:

$$q_{mod}(\omega) = \frac{p_i(\omega) - p_0(\omega)}{max_\omega(p_0(\omega))} \tag{7}$$

$q_{mod}(\omega) > 0$ ($q_{mod}(\omega) < 0$) denotes constructive (destructive) interactions. When the q-factor and the q_{mod}-factor are computed over a set of N_b bodies, $p_i(\omega)$ and $p_0(\omega)$ are replaced by $\sum_i^{N_b} p_i(\omega)$ and $N_b.p_0(\omega)$ in Eqs. (6) and (7). We also consider the yearly averaged power output as defined in Eq. (5). This value will be noted Pyr_{R_i} and Pyr_A when averaged on the row i of the WEC array and on the whole WEC array, and Pyr_0 for an isolated WEC. In all the plots related to Pyr, the scale is chosen to emphasize the tendencies of interactions effects. It is important to check the vertical axis to properly evaluate their magnitude.

3.1. PTO for optimal yearly energy production

3.1.1. Triangle based WEC arrays

Surging barges: We start considering the central WEC of 9-body arrays (body 5, situated in the 2nd row and in the 2nd column), for different separating distances dx. According to Fig. 4(a), the body is influenced by its neighbours for a large range of wave periods. Considering the q_{mod}-factor (Fig. 4(b)) shows the same tendency, as the WEC is a large-banded (with a significant power production for a large spectrum, see Fig. 1(a)). However, there are strong variations from one wave period to another. The shapes of the q_5-factor and of the $q_{mod\,5}$-factor (q-factor and q_{mod}-factor at body 5) strongly depend on dx.

Considering the full range of dx values, the dependency of the q_{mod}-factor and Pyr on dx are investigated. Fig. 5(a) shows that over the studied range of periods, constructive interactions dominate in the three rows of the WEC arrays. The calculation of Pyr "aggregates" these constructive and destructive interactions over the year, so variations of Pyr depending on dx are smooth (Fig. 5(b)). In this figure, one can see that energy absorption is increased in the WEC array in comparison with isolated WECs. This is interesting information for the WEC arrays designer: even if the energy gain is low, such a configuration ensures at least that destructive interactions will be cancelled. The plot in Fig. 5(b) underlines several tendencies:

- For the smallest values of dx, the 3rd row of WECs suffers from negative interactions. Indeed WECs from the 1st and 3rd rows are aligned. With dx small, the 1st row masks the waves to the 3rd row.

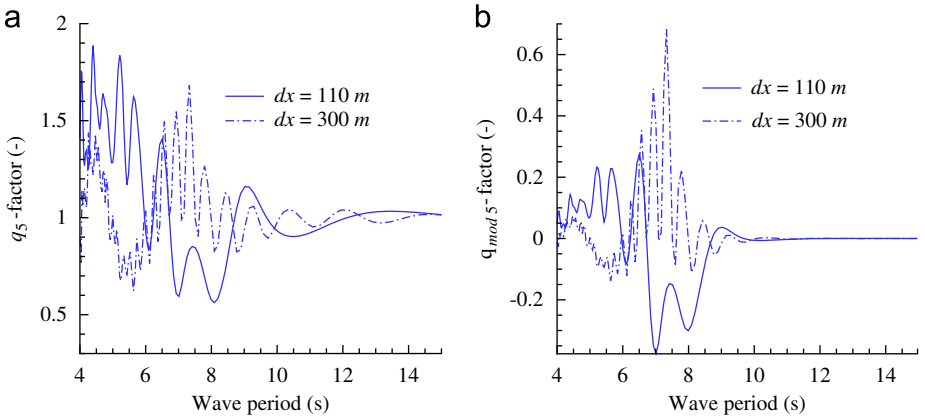

Fig. 4. Interaction factors (q_5- and $q_{mod\,5}$-factor) at the central WEC (body 5) of 9-body arrays of surging barges with different separating distances dx ($b_{pto} = b_{pto\,yr}$). (a) q-factor and (b) q_{mod}-factor.

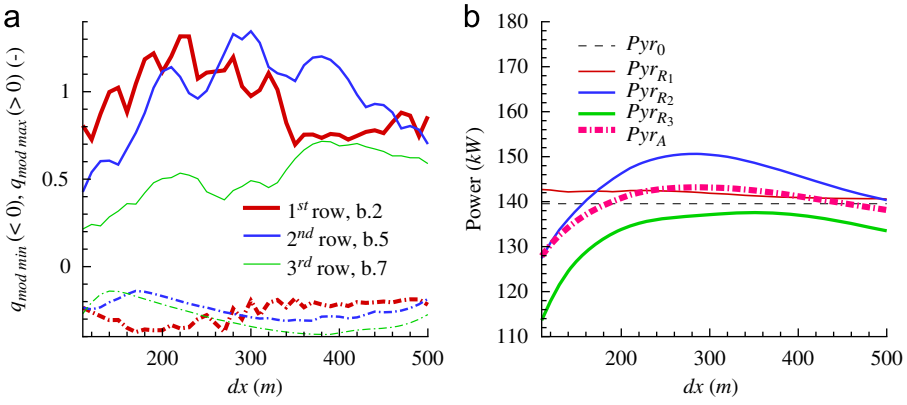

Fig. 5. Interaction factors ($q_{mod\,min}$- and $q_{mod\,max}$-factor) and power production of 9-body triangle-based arrays of surging barges ($b_{pto} = b_{pto\,yr}$), (a) Min. values (dashed lines) and max. values (solid lines) of the q_{mod}-factor over the wave period range, at rows centers (bodies 2, 5, 7). and (b) Yearly averaged power output.

- The 1st row of WECs benefits from constant positive interactions. The nearly flat shape of the curve suggests that the 1st row of WECs is almost not impacted by the rest of the WEC array (especially because it does not suffer from masking effects). The two last rows of WECs act as reflectors sending waves back to the 1st row, which explains the positive interactions.
- The 2nd row of WECs has the highest power production, as it is nearly unmasked and benefits from waves radiated by the two other rows.
- The convex shape of Pyr_{R_2}, Pyr_{R_3} and Pyr_A suggests that triangular grids might not be the best configuration for finding a compromise between the limitation of masking effects and the harnessing of waves radiated by neighbouring WECs.

The last point is clearly underlined in Fig. 6, where *dx* and *dy* are independent from each other (2-parameter study). It shows that the most beneficial interactions occur if a roughly linear relation between *dx* and *dy* is respected. The triangle-based arrays case goes across the zone of positive interactions, which explains the convex shape of Pyr_A on Fig. 5(b). The same tendencies occur for 16- and 25-body triangle-based arrays of surging barges (Fig. 7), with the masking effect being more important the more rows of WECs. As a consequence of this effect, the overall constructive interactions cannot be maintained for arrays having more than three rows. For most cases, interactions tendencies for 9-body arrays are the same for 16- and 25-body arrays; thus mainly 9-body arrays results will be presented.

Heaving cylinders: Results in Fig. 8(b) show similar tendencies as previously. The convex shape of the curves is less marked than for the surging barges, probably because the WECs are axisymmetric and can more easily catch wave radiated by surrounding WECs. The maximum gain provided by wave interactions is only 1% (at $dx=450$ m). A quick "2-parameter study" is carried on, to sweep the values of *dx* and *dy* separately. Its results on Fig. 9 show the same tendency of balance between masking effect and radiation sharing than for the surging barges case. The sensitivity to *dy* is lower, probably because heaving cylinders have a lower absorption, leading to limited masking effect. Fig. 8(a) suggests that a large *dx* increases positive interactions at large wavelengths, where most of the energy is. However, the results of Fig. 8(a) are difficult to read: interactions are more complex when the separating distance increases. This is due to the fact that the range of wavelengths at which significant interactions can occur is larger. Note that positive interactions for two aligned surging barges are also found in Babarit (2010) at large distances ($dx=2000$ m).

3.1.2. Square based WEC arrays

The behaviour of square-based arrays depends much more on the WEC type than for triangle-based arrays. As surging barges are more efficient WECs, there are significant masking effects between aligned WECs (Fig. 10(a)). This leads to strong discrepancies in energy absorption between different rows of WECs. The 1st row benefits from waves sent back by other rows. For heaving cylinders,

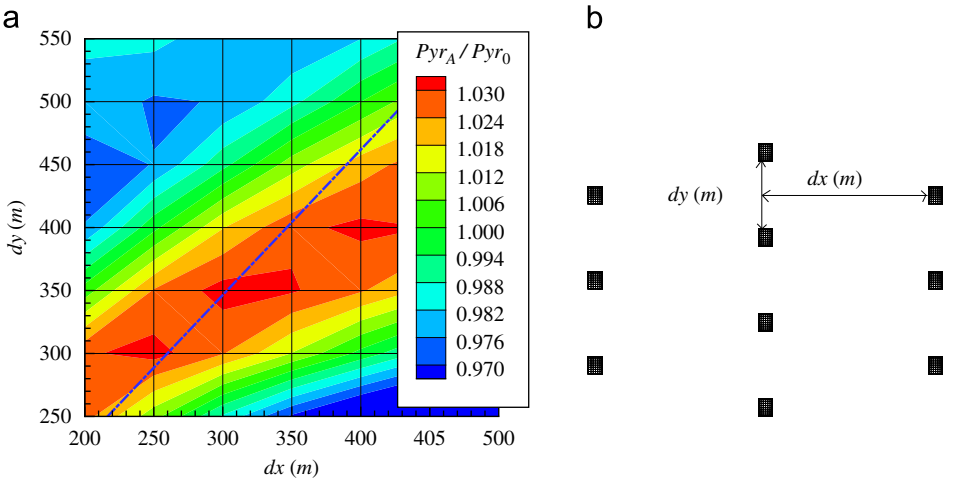

Fig. 6. Power production of 2-parameter arrays of 10 surging barges ($b_{pto} = b_{pto\ yr}$). (a) Pyr_A/Pyr_0 (dashed line: triangle-based arrays) and (b) 2-parameter arrays.

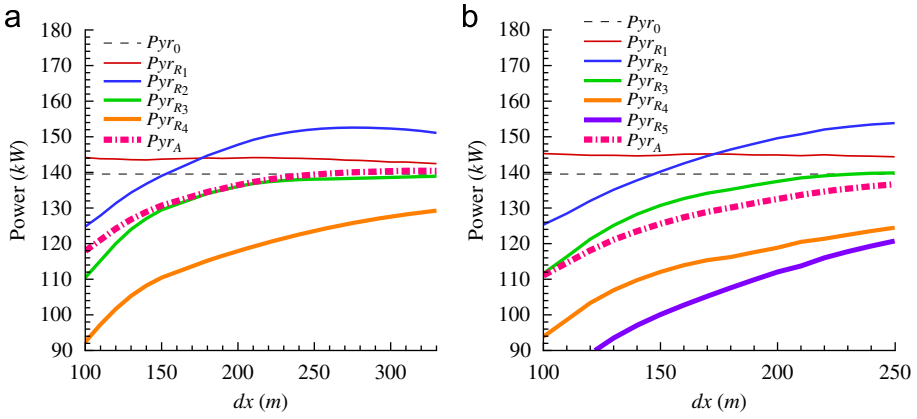

Fig. 7. Yearly averaged power for triangle-based arrays of surging barges ($b_{pto} = b_{pto\ yr}$): (a) 16-bodies and (b) 25-bodies.

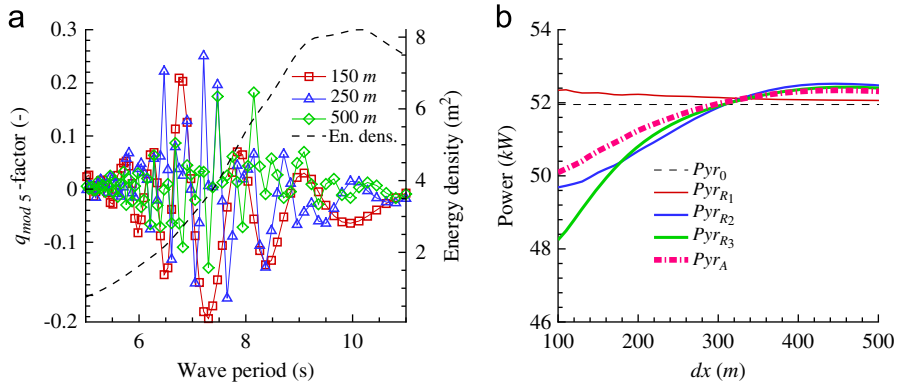

Fig. 8. Interaction factors ($q_{mod\ 5}$-factor) and power production of 9-body triangle-based arrays of heaving cylinders ($b_{pto} = b_{pto\ yr}$). (a) q_{mod}-factor depending on dx and (b) yearly averaged power output.

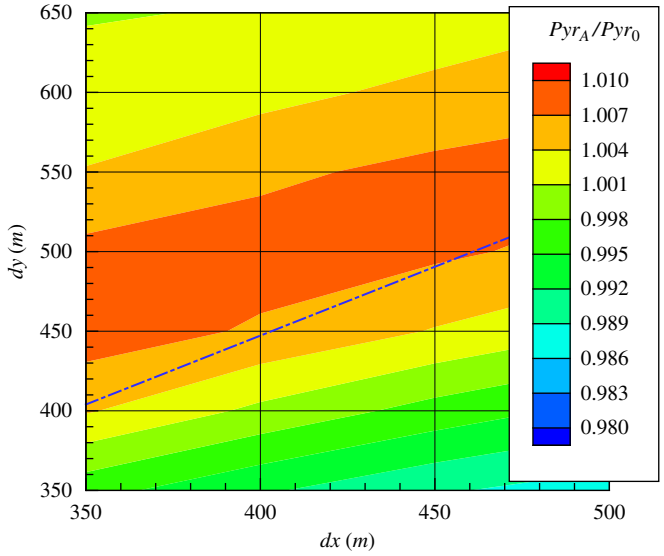

Fig. 9. Pyr_A/Pyr_0 for 2-parameter WEC arrays of 10 heaving cylinders with $b_{pto} = b_{pto\ yr}$. (dashed line: triangle-based arrays.)

a maximum in the WEC array production can be found for around dx=180 m. Interactions are always positive at the WEC array scale; their influence on power production slowly diminishes as dx increases. The masking effect on the 3rd row of WECs quickly disappears. Two reasons explain this behaviour:

- The heaving cylinders are less efficient than the surging barges, leading to a limited masking effect.
- Heaving cylinders are axisymmetric WECs, so positive interactions are more likely to occur between WECs directly aligned. These interactions are stronger for the 2nd row of WECs, whose bodies have more neighbouring WECs.

Simulations with 16 (Fig. 11) and 25 bodies (not represented) show the same tendencies for the two types of WECs, with increased masking effects on the last rows.

3.1.3. Optimizing $b_{pto\ yr}$ for the WEC array

In an attempt to improve energy production, an optimal b_{pto} for the WEC array (instead of optimal for an isolated body) has been looked for. For triangle-based arrays of surging barges and square-based arrays of heaving cylinders (and for each value of dx), values of b_{pto} have been changed and equally applied to all the bodies until reaching a maximum in Pyr_A. Unlike in De Backer et al. (2009) (where the optimal b_{pto} is investigated for closely spaced bodies), the optimal damping is the same for isolated bodies or bodies in a WEC array. This underlines relatively low interaction effects, due to the long separating distances and low motion amplitudes.

3.2. PTO optimal at resonant frequency

3.2.1. Square based WEC arrays

Heaving cylinders: We consider the central WEC of 9-body arrays (body 5). Fig. 12(a), shows interactions over a large range of wave periods. Considering the q_{mod}-factor on Fig. 12(b) filters these results; significant interactions only occur near the resonant wave period, where the maximum power output is reached for isolated WECs (Fig. 1(a)). At $T \approx 7.3$ s, the WECs are likely to have their maximum motion amplitude (Fig. 1(b)), leading to strong radiation and significant interactions. Fig. 12(b) clearly shows constructive interactions for the central body (body 5) at dx=150 m and dx=330 m, and destructive interactions at dx=270 m.

A strong dependency of the q_{mod}-factor and of Pyr (Fig. 13) on dx is found. A correlation is visible between maximum of the q_{mod}-factor ($q_{mod\ max}$) and Pyr for each row of the WEC array. The WEC being narrow-banded makes it more sensitive to dx than in the case where a PTO tuned for optimal yearly production is chosen (see Section 3.1). This is because constructive and destructive interactions no longer compensate over the wave period range (Fig. 12(b)). Fig. 13(b) shows that Pyr_A oscillates around the output of an isolated WEC. The 2nd row of WECs is the one which is the most influenced by interactions. Considering 16- and 25-body arrays (Fig. 14) shows that the three 1st rows of WECs are almost not influenced by the presence of the 4th and 5th rows of WECs, and behave as an independent entity (the last rows then suffering from strong masking effects).

Child and Venugopal (2009) established that for a given wave period, optimal WEC arrays can be designed by placing WECs in points where the incident waves are in phase with the waves radiated by other bodies. Here most of the energy is produced at $T \approx 7.3$ s (narrow-banded WECs), so this reasoning can be used even considering Pyr. Fig. 15 shows the wave amplitude (considering radiated, diffracted and incident waves) at resonance around one heaving cylinder and three heaving cylinders facing the incident waves. A 9-body array (dx=150 m) is represented over this wave field. Neglecting body interactions as a first approximation, Fig. 15(a) shows that dx=150 m situates the bodies at the mentioned 'phase points'. In the same way, Fig. 15(b) shows that the 1st and 2nd rows of WECs benefit from waves sent back by the 3rd row. Fig. 15 suggests a high sensitivity to dx and dy, which has

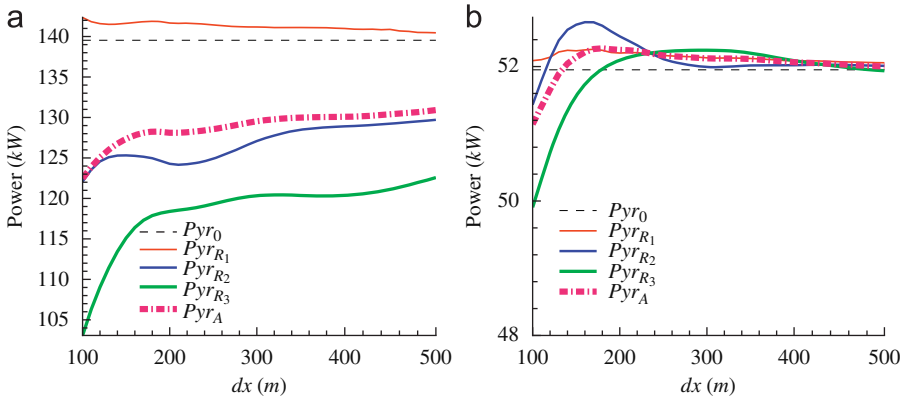

Fig. 10. Power production of 9-body square-based WEC arrays ($b_{pto} = b_{pto\ yr}$). (a) Surging barges and (b) heaving cylinders.

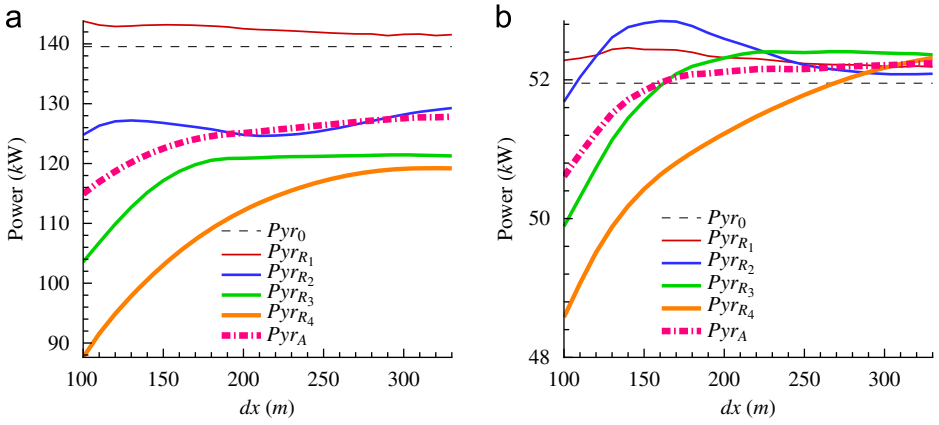

Fig. 11. Power production of 16-body square-based WEC arrays ($b_{pto} = b_{pto\ yr}$). (a) Surging barges and (b) heaving cylinders.

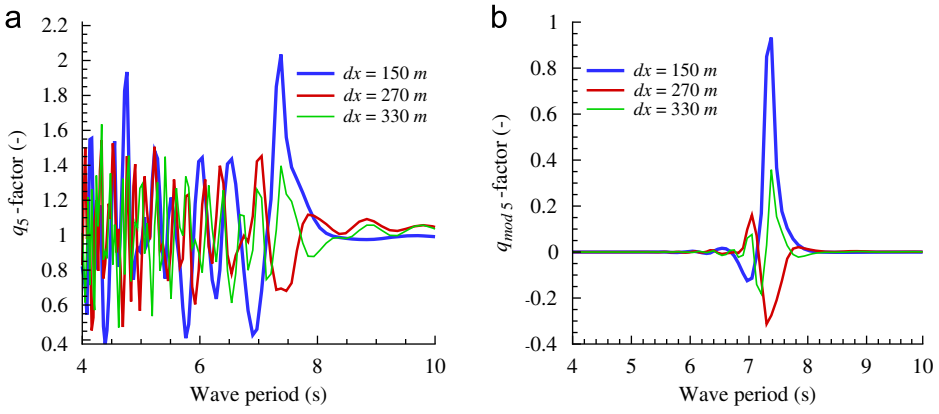

Fig. 12. Interaction factors (q_5- and $q_{mod\ 5}$-factor) at the central WEC (body 5) of 9-body square-based arrays of heaving cylinders ($b_{pto} = b_{pto\ \omega_0}$). (a) q-factor and (b) q_{mod}-factor.

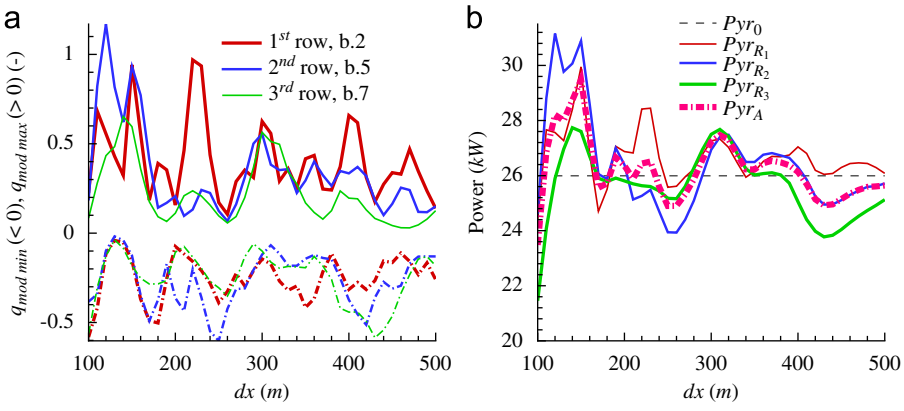

Fig. 13. Interaction factors ($q_{mod\ min}$- and $q_{mod\ max}$-factor) and power production of 9-body square-based arrays of heaving cylinders ($b_{pto} = b_{pto\ \omega_0}$). (a) Min. values (dashed lines) and max. values (solid lines) of the q_{mod}-factor over the wave period range, at rows centers (bodies 2, 5, 7). and (b) Yearly averaged power output.

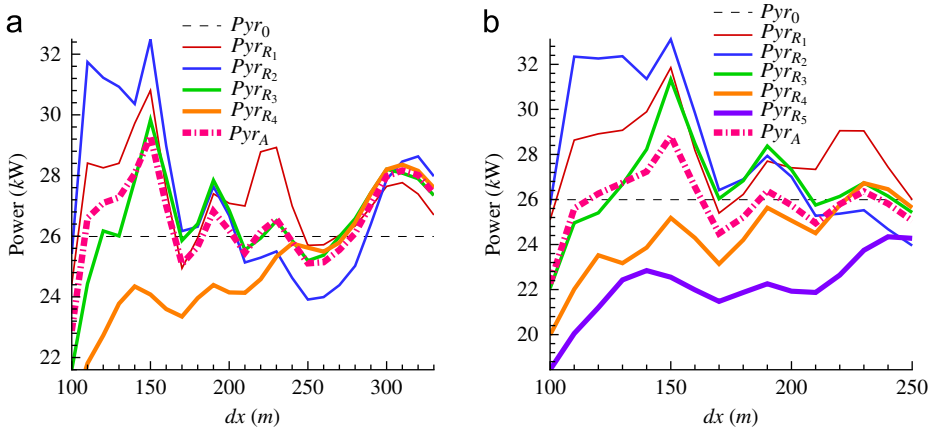

Fig. 14. Power production of square-based arrays of heaving cylinders ($b_{pto} = b_{pto\ \omega_0}$). (a) 16-bodies and (b) 25-bodies.

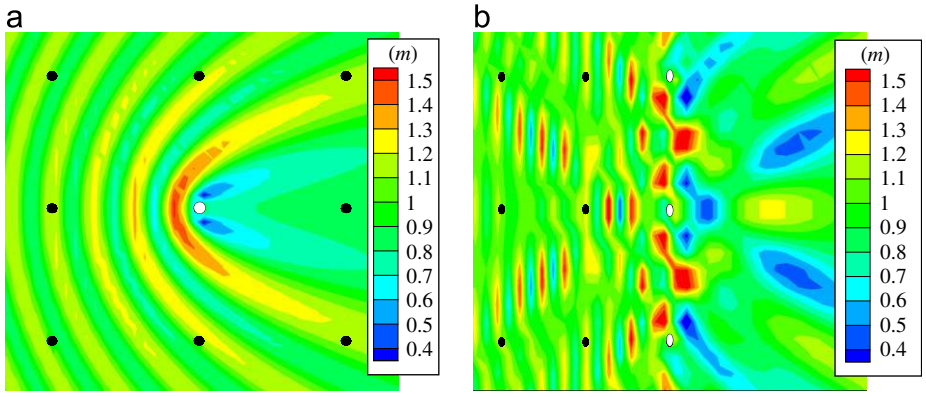

Fig. 15. Wave amplitude (m) at $T = 7.3\,s$ around a set of 1 (a) or 3 (b) heaving cylinders and view of a 9-body array (a,b). Waves coming from the left, $b_{pto} = b_{pto\ \omega_0}$. (a) Wave amplitude around the white cylinder and (b) wave amplitude around the three white cylinders in interaction.

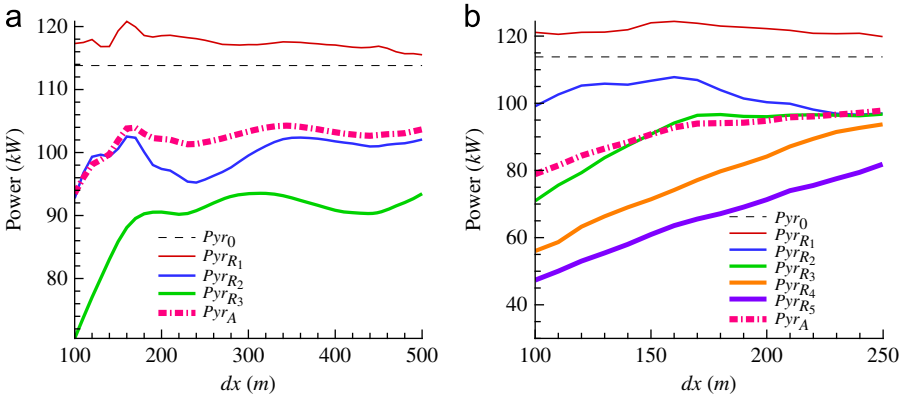

Fig. 16. Power production of square-based arrays of surging barges ($b_{pto} = b_{pto\ \omega_0}$): (a) 9-bodies and (b) 25-bodies.

be confirmed by a 2-parameter study around $dx,dy \approx 150$ m (not shown here).

Surging barges: The WECs having a narrower bandwidth than in the case of a yearly optimized PTO (see Section 3.1.2), Fig. 16 shows a less steady evolution of *Pyr* according to *dx* (but still very steady compared to the heaving cylinder case). The WECs extracting more power at the resonance, the masking effect is stronger and leads to higher discrepancies between rows of WECs.

3.2.2. Triangle based WEC arrays

Heaving cylinder: In Fig. 17, P_{yr} and the q_{mod}-factor for triangle-based arrays show a very high dependency on *dx*, looking periodic. This is similar to what can be found for square-based arrays (see Fig. 13). However, once again for the triangle-based arrays, a "convex" curve can be found in average for the WEC array production, revealing a balance between negative and positive interactions at large distances.

Surging barges: The behaviour of the surging barges with $b_{pto\ \omega_0}$ is relatively similar to that with $b_{pto\ yr}$. As a consequence, the same tendencies are found for both cases for triangle-based arrays.

4. Conclusion

Tables 3 and 4 summarize this study results, showing the extreme values of energy gains (or losses) that can be expected

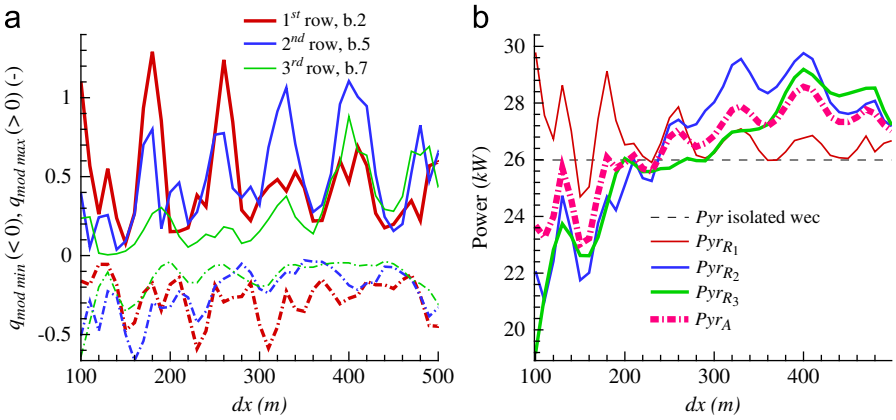

Fig. 17. Interaction factors ($q_{mod\ min}$-and $q_{mod\ max}$-factor) and power production of 9-body triangle-based arrays of heaving cylinders: (a) Min. values (dashed lines) and max. values (solid lines) of the q_{mod}-factor over the wave period range, at rows centers. and (b) Yearly averaged power output.

Table 3
Max. and min. values of $100 \cdot (Pyr_A - Pyr_0)/Pyr_0$ for 9-body arrays with $b_{pto} = b_{pto\ yr}$. Bold numbers show the array configuration and WEC type for which Pyr_A is the highest.

Array	Device	dx	Min.	dx	Max.
Square	Cylinder	100	−1.5	180	0.6
Triangle	Cylinder	100	−3.6	450	**0.7**
Square	Barge	100	−11.9	500	−6.2
Triangle	Barge	100	−7.7	280	**2.6**

Table 4
Max. and min. values of $100 \cdot (Pyr_A - Pyr_0)/Pyr_0$ for 9-body arrays with $b_{pto} = b_{pto\ \omega_0}$. Bold numbers show the array configuration and WEC type for which Pyr_A is the highest.

Array	Device	dx	Min.	dx	Max.
Square	Cylinder	100	−8.9	150	**13.4**
Triangle	Cylinder	150	−11.4	400	9.9
Square	Barge	100	−17.6	340	−8.4
Triangle	Barge	100	−12.9	350	**7.9**

when the WECs separation distance is between 100 m and 500 m for the investigated WECs. The energy production is always larger when $b_{pto} = b_{pto\ yr}$.

This generic study gives an insight on the behaviour of WEC arrays, and permits to draw guidelines for designing an array. First, large-banded WECs should be chosen. This way interactions occur over a significant portion of the wave period range. When summed together over a yearly spectrum, interactions compensate each other and the overall energy output steadily evolves with the separating distance between WECs. This gives much more flexibility in the array design, permitting to take other issues (mooring, access for maintenance…) into account more easily.

The PTO damping value must be chosen considering the yearly energy production, rather than the power at resonant frequency. Large damping values are interesting, as they limit the motions of the WECs and the resulting radiation. Consequently, the influence of wave interactions is reduced. Narrow-banded WECs with low PTO damping values must be avoided, as the power output is strongly dependent on the spacing, and could be badly impacted by the drift of WECs or improper array building.

When the WECs are very efficient, choosing square-based arrays is not appropriate (especially for short separating distances), as strong masking effect occur. Triangle-based arrays, or better, arrays described by two parameters (*dx*,*dy*) are the best configuration, as they permit to reach an optimum between masking effect (destructive interactions) and the WECs sharing each other radiation (constructive interactions). Note that the square-based array can give good results for axisymmetric WECs having positive side-side interactions.

In general, considering yearly energy production shows that negative and positive interactions compensate each other, and that the positioning on the WECs is not a major issue, since the above recommendations are satisfied. The effect of interactions on energy extraction is rather limited, considering the approximations and hypothesis involved in this model. Thus, the WEC array designer has some flexibility in the positioning of the WECs, regarding other constraints (available area, mooring configuration …). These constraints can be satisfied with a minor impact on the yearly energy absorption.

Several investigations are still necessary to have a better insight on WEC arrays, including the effect of directional wave spreading, studies on arrays described by more than two distance parameters (*dx*,*dy*), the effect of disorder in the WECs positioning, due to improper installation, or to second order drift forces.

References

Babarit, A., 2010. Impact of long separating distances on the energy production of two interacting wave energy converters. Ocean Eng. 37, 718–729.

Bellew, S., Stallard, T., Stansby, P., 2009. Optimization of heterogenous array of heaving bodies. In: Proceedings of the 8th Wave and Tidal Energy Conference, Uppsala, Sweden.

Borgarino, B., Babarit, A., Ferrant, P. An implementation of the fast multipole algorithm for wave interactions problems on sparse arrays of floating bodies, J. Eng. Math., submitted for publication.

Budal, K., 1977. Theory for absorption of wave power by a system of interacting bodies. J. Ship Res. 21 (4), 248–253.

Child, B.F.M., Venugopal, V., 2009. Modification of power characteristics in an array of floating wave energy devices. In: Proceedings of the 8th European Wave and Tidal Energy Conference, Uppsala, Sweden.

Cruz, J., Sykes, R., Siddorn, P., Eatock-Taylor, R., 2009. Wave farm design: preliminary studies on the influences of wave climate, array layout and farm control. In: Proceedings of the 8th European Wave and Tidal Energy Conference, Uppsala, Sweden.

De Backer, G., Vantorre, M., Beels, C., De Rouck, J., Frigaard, P., 2009. Performance of closely spaced point absorbers with constrained floater motion. In: Proceedings of the 8th European Wave and Tidal Energy Conference, Uppsala, Sweden.

Delhommeau, G., 1993. Seakeeping codes Aquadyn and Aquaplus. In: Nineteenth WEGMENT School, Numerical Simulation of Hydrodynamics: Ship and Offshore Structures.

Falnes, J., 1984. Wave-power absorption by an array of attenuators oscillating with unconstrained amplitudes. Appl. Ocean Res. 6 (1), 16–22.

Falnes, J., 2002. Ocean Waves and Oscillating Systems. Cambridge University Press.

Falnes, J., Budal, K., 1982. Wave-power absorption by parallel rows of interacting oscillating bodies. Appl. Ocean Res. 4 (4), 194–207.

Filtzgerald, C., Thomas, G., 2007. A preliminary study on the optimal formation of an array of wave power devices. In: Proceedings of the 7th European Wave and Tidal Energy Conference, Porto, Portugal.
Folley, M., Whittaker, T., 2009. The effect of sub-optimal control and the spectral wave climate on the performance of wave energy converter arrays. Appl. Ocean Res. 31, 260–266.
Garnaud, X., Mei, C., 2009. Comparison of wave power extraction by a compact array of small buoys and by a large buoy. In: Proceedings of the 8th European Wave and Tidal Energy Conference, Uppsala, Sweden.
Greengard, L., 1988. The Rapid Evaluation of Potential Fields in Particle Systems. MIT Press.
Justino, P., Clement, A., 2003. Hydrodynamic performance for small arrays of submerged spheres. In: Proceedings of the 5th European Wave Energy Conference, Cork, Ireland.
Ricci, P., Saulnier, J., Falcao, A., 2007. Point-absorbers arrays: a configuration study off the Portuguese west-coast. In: Proceedings of the 7th European Wave and Tidal Energy Conference, Porto, Portugal.
Saad, Y., Schultz, M.H., 1986. GMRES: a generalized minimal residual algorithm for solving nonsymmetric linear systems. SIAM J. Sci. Statist. Comput. 7, 856–869.
Thomas, G., Evans, D., 1981. Arrays of three-dimensional wave-energy absorbers. J. Fluid Mech. 108, 67–88.